Some Results from 1/8-Scale Shuttle Model Vibration Studies

Larry D. Pinson* and Sumner A. Leadbetter*
NASA Langley Research Center, Hampton, Va.

Highlights of experimental and analytical vibration studies of a 1/8-scale structural dynamic model of the space shuttle are presented. The space shuttle is a launch vehicle with elements assembled in an asymmetric manner. Responses of the assembled vehicle are characterized by directional coupling and high modal density at low frequencies. Effects of distortion of structure near element interfaces are shown to be significant and predictable with highly detailed mathematical models. Acquisition of modal data by single-point random excitation is shown to be viable for these complex structures. Element studies reveal large liquid-structure interactions and a wide range of structural damping.

Introduction

THE structural dynamic characteristics of launch vehicles are fundamental inputs required for assessing dynamic loads on the structure, crew, and cargo resulting from gusts, ignition, and staging transients. These characteristics are also necessary for assessment of control system effectiveness and control system stability associated with structural feedback, aeroelastic stability (flutter), and structure-propulsion system stability (pogo). Structural dynamic characteristics usually are specified as natural frequencies, mode shapes, and damping. In liquid-propelled launch vehicles these structural dynamic characteristics also include those modes in which contained liquids interact significantly with the structure.

Although the adequacy of prediction methods has been continually assessed by flight tests during the evolution of launch vehicles, there is no guarantee that methods are satisfactory for new vehicle designs featuring configurations which differ significantly from those of previous designs. However, a sufficient degree of confidence in the analysis can be established early in the vehicle design process through the use of subscale dynamic models.[1,2] In support of the development of space launch systems, several structural dynamics model investigations have been conducted to provide early test data for evaluation of analytical procedures[3-7] and gain understanding of vehicle structural dynamics behavior. A similar effort was undertaken to understand more fully the developing space shuttle launch vehicle.

A comprehensive and early dynamic model program was particularly important for the space shuttle because of its unique configuration. Four large structural elements are joined asymmetrically at a few discrete interfaces in contrast to prior launch vehicles which were relatively slender and nearly axisymmetric. Thus, unusual effects for launch vehicle structural dynamics are present with various combinations of pitch, yaw, axial, and roll coupling occuring.

To assess analytical modeling procedures and provide test data with which to understand the dynamic behavior of shuttle-like configurations, a 1/8-scale dynamic model of an early shuttle four-body concept was built for structural dynamics investigations. Comprehensive structural dynamics tests and analyses were performed.

Analysis was assessed for efficient finite-element modeling prediction of liquid-structure interaction and model interface definition for component coupling. The purpose of this paper is to present significant results of these model investigations. A brief description of the 1/8-scale model is given, the methods of vibration testing are described, and a brief definition of analytical models and comparisons of analysis and experimental results are made.

Presented as Paper 77-407 at the AIAA 18th Structures, Structural Dynamics and Materials Conference, San Diego, Calif., March 21-23, 1977; submitted Dec. 5, 1977; revision received July 12, 1978.

Index category: LV/M Vibration.

*Aerospace Engineer. Member AIAA.

Model Description

Various aspects of the 1/8-scale model are depicted in Figs. 1 and 2. The assembled model is shown in Fig. 1. The model is comprised of four major elements (Fig. 2): a large propellant tank called the external tank (ET), two solid rocket boosters (SRB), and an airplane-like orbiter. The interstage loading directions between elements are shown in Fig. 3. Model interstages are similar to those on the full-scale structure. Both SRB's and the orbiter are attached to the ET in a statically determinate manner. The assembled configuration has one plane of symmetry, the pitch (x-z) plane. Each model element is described briefly below. Element masses in the liftoff configuration are indicated in Fig. 2. Additional model construction details are given in Refs. 8-14.

External Tank (ET)

The ET has four components: a liquid oxygen (lox) tank, an intertank skirt, a liquid hydrogen tank, and an aft skirt. The lox tank is an unstiffened aluminum shell structure (Fig. 2) that includes a forward truncated conical section, a central cylindrical section, and an aft dome. Water is used to simulate

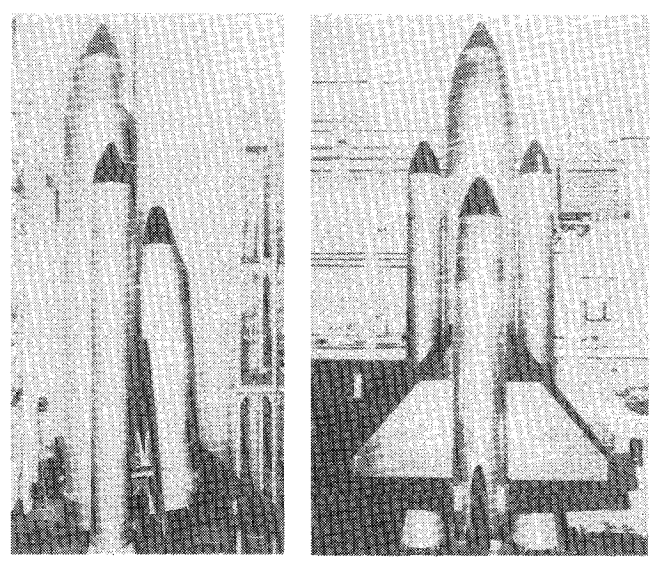

Fig. 1 One-eighth scale space shuttle structural dynamics model.

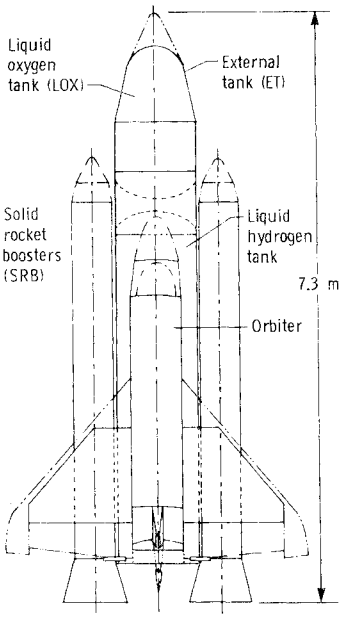

Fig. 2 Model nomenclature and mass.

Element	Percent of total mass at liftoff[a]
Solid rocket boosters (2)	59
External tank	36
Orbiter	5

[a] Model liftoff mass is 3975 kg

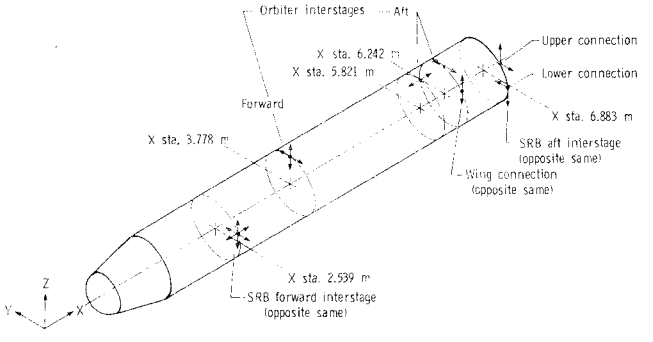

Fig. 3 Model attachment loading directions.

lox. The depth of water in the lox tank was varied to simulate various flight mass conditions.

Both the full-scale and model lox tanks are essentially unstiffened shells containing liquid; a characteristic which allows very complex modes to exist in the frequency range of interest. However, construction of the model lox tank differs from that of the full-scale tank in three respects. First, the forward section of the full-scale tank is a ogive-shaped shell of revolution whereas the model tank is conical. Second, the full-scale tank has a slosh baffle assembly not represented in the model. The full-scale tank baffle attaches to the tank at the ends of the cylindrical section and is ineffective for suppression of shell dynamic response. Third, a portion of the cylindrical section of the full-scale tank is nonaxisymmetric in stiffness due to local stiffening near the ET-SRB interface.

The model intertank skirt, similar to the full-scale structure, a ring-stiffened cylinder, contains the forward SRB-ET interstage connections. Additional stiffening provided near these connections renders the structure nonaxisymmetric in stiffness.

The model liquid hydrogen tank is similar to the full-scale structure, a ring-stiffened aluminum cylinder with domes. This component contains the connections for the orbiter attachment. Again, local stiffening is provided near the interstage connections. The liquid hydrogen is simulated with

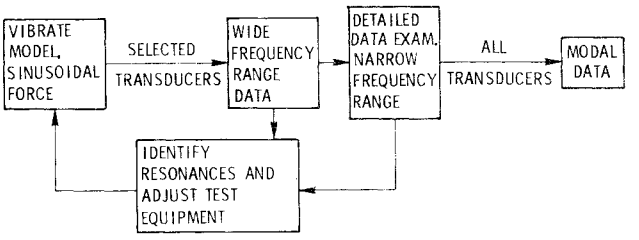

a)Sinusoidal test

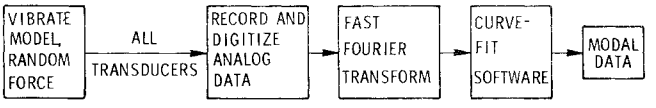

b) Single-point random excitation test

Fig. 4 Vibration test procedures for model test program.

small plastic pellets having the same specific gravity as liquid hydrogen (0.071). The aft skirt is a ring-stiffened aluminum cylinder. A detailed description of the ET elements is given in Refs. 8-10.

Solid Rocket Boosters (SRB's)

Three pairs of SRB's simulate configuration mass at three flight times: liftoff, midburn, and near-burnout. The model propellant is the same as the flight propellant except for the replacement of the oxidizer with a salt to make the mixture inert. Three aluminum alloy components make up an SRB: a forward skirt, a propellant bonded to the inside wall, and an aft skirt section. Attachments to the ET are contained in the forward and aft skirts. Of these components, only the propellant cylinder is axisymmetric. Further details may be found in Refs. 8 and 12.

Orbiter

The orbiter element is a riveted aluminum alloy structure consisting of thin, nontapered skins with supporting frames and longerons. Consistent with the full-size structure, model construction is such that bending loads in the orbiter are not resisted by the cargo-bay door, but the door is effective in torsion. Wings are standard rib-spar-skin construction with ballast masses attached internally to the stiffeners to achieve the proper scaled mass. Concentrated masses are used to represent the orbital maneuvering system in the aft end and nonstructural mass in the crew cabin area. Detailed descriptions of the orbiter element are presented in Refs. 11 and 13.

Vibration Test Methods

Vibration tests of the ⅛-scale shuttle dynamic model, both for the individual elements and the assembled model, were conducted with simulated free-free boundary conditions.[14] Test procedures shown in Fig. 4 were used to obtain the modal characteristics of the dynamic model. The sinusoidal test approach (Fig. 4a) was used to obtain most of the structural dynamics data. The single-point random excitation test approach (Fig. 4b), a relatively new test technique, was used during limited tests to study the adequacy of such a random force test method.

Sinusoidal Tests

During the sinusoidal tests depicted on Fig. 4a, the model was vibrated using either one or two exciters (with a low input sinusoidal force ranging from 2-9 N) over a relatively wide frequency range, 12-150 Hz, while data were obtained from a limited number of transducers. Generally, resonant frequencies were identified while monitoring the output from selected transducers by means of amplitude-phase, co-quad or Kennedy-Pancu data interpretation techniques.[14-17] Modal data were obtained during dwell tests in the vicinity of resonant frequencies. Modes that were relatively well defined

were identified immediately and pertinent data were recorded. Modes that were unclear or at closely spaced frequencies required additional test effort. When local responses, for example, panel resonances, and modes of interest were at nearly the same frequency, it was necessary to suppress the local responses by means of added mass or stiffness or to relocate exciters such that the needed mode was isolated for measurement. In instances where a complex response involved multiple elements or directions, it was necessary to locate exciters at specific model locations and orientations to obtain satisfactory modal data. For example, to minimize a given mode, exciters were located near a node for that mode. Once a modal frequency and the associated response characteristics were adequately identified, detail structural dynamic data were measured using all transducers (94 in the liftoff configuration). Orthogonality was not used to evaluate modal purity. Instead, clean single-mode decay, co-quad techniques, and acceptable Kennedy-Pancu plots were obtained and utilized as criteria for acceptable modal data.

Single-Point Random Excitation

Only the assembled dynamic model representative of the liftoff configuration was excited by single-point random force. For this random input force, an electrodynamic shaker was attached at an intermediate angle to a solid rocket motor aft skirt, and a random force, approximately 16 N rms with a flat power spectrum over a frequency range of 10 to 200 Hz, was applied to the model. All transducer output signals were recorded on analog tape. The analog data were converted to digital form and frequency-domain data were obtained by means of the Fast Fourier Transform. These data were then analyzed by means of a curve-fitting procedure to extract modal data.[18]

Analysis

Efforts to ascertain and evaluate methods appropriate for analysis of shuttle-like configurations involved mathematical models of varying types and complexity for the ⅛-scale shuttle model elements. Initially, each element was modeled using the current (level 15) NASTRAN finite-element structural analysis computer program. Consistent with the shuttle project plans, these component finite-element models were intended to be combined to analyze the mated vehicle characteristics at various flight times or mass conditions. Although the orbiter finite-element model proved to be valuable, prohibitively large mathematical representations of the ET and SRB would have been required to model important local deformations near element interfaces. As a consequence, simple beam-type models were derived for the ET and SRB elements with local effects accounted for by springs obtained from detailed static analysis. Herein, the more complex finite-element model is referred to simply as the finite-element model. Typical numbers of degrees of freedom for the finite-element and beam models are shown in Table 1 to indicate the degree of detail in these models.

Local flexibilities are important for an adequate understanding of the structural dynamic characteristics of the two- and four-body mated vehicle configurations. In an effort to arrive at a better understanding of the element dynamic properties, static tests of the elements were conducted and correlated with results of analysis where the finite-element models, modified to have much greater detail in the structure surrounding the interface, were used. From these static load studies, spring representations of the model interface dynamic properties were derived analytically for use with the beam models of the elements during mated vehicle analysis-test studies.

The finite-element and beam models are discussed herein. In addition, improvements in the NASTRAN fluid-structure interaction analysis are discussed along with a shell-of-revolution analysis which was modified to study the fluid-filled lox tank.

External Tank

The finite-element model of the external tank is shown in Fig. 5a. This finite-element model contains elements representing all rings, other internal stiffening members, and asymmetries present in the ⅛-scale test article. As a compromise between a reasonable representation of the simpler shell modes and the necessity to reduce the size of the mathematical model, flat plate elements subtending 22½ deg of circumference were used for the span of each element yielding 9 grid points about a semicircumference. Quadrilateral and triangular bending and membrane elements were used to simulate the remainder of the ET structure. The fluid model describes the dynamics of the contained fluids and was selected to describe asymmetric dynamics with the pitch plane taken as the plane of symmetry.

When the contained fluid was incorporated into the mathematical model by using the hydroelastic analysis capability of NASTRAN, the resulting model was excessively large and unacceptable. A significant improvement was made in NASTRAN capability as a result.[19] Acceptable correlation with lower frequency modes could then be obtained. However, more complex shell modes still could not be computed accurately. In addition, a standard beamtype model with fluid branch masses was developed which also provided acceptable correlation with lower frequency modes. Consequently, this beamtype model was used in mated model studies. For longitudinal vibrations, the conventional single-degree-of-freedom fluid representation[6] was inadequate. A more complex axisymmetric shell-liquid program,[20] was used to predict the dynamic behavior in correlation with experimental results.

In addition, to address more directly the primary source of difficulty in the correlation study with experimental data, separate investigation of the isolated liquid hydrogen tank was conducted. An existing shell-of-revolution computer program, known as SRA, was modified to accept contained fluids.[21]

Solid Rocket Boosters

The finite-element model is shown in Fig. 5b and is further detailed in Refs. 9 and 12. The outer shell or case is modeled with finite-element flat plates, each of which includes 30 deg

Table 1 One-eighth-scale shuttle mathematical model degrees of freedom

Element	Initial NASTRAN model		Mated model beam analysis
	Before Guyan reduction	After Guyan reduction	
Orbiter (symmetric half model)	2469	339	181
External tank (symmetric half model)	1872	412	65
Lox tank (symmetric half model)	766	196	...
Solid rocket booster	3114	212	114

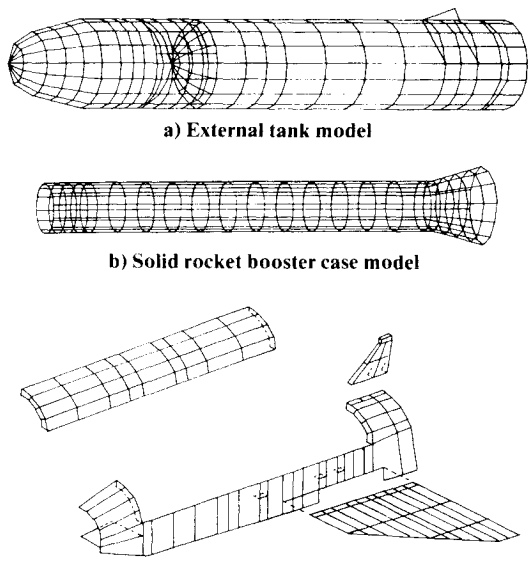

a) External tank model

b) Solid rocket booster case model

c) Reduced orbiter model

Fig. 5 NASTRAN models of elements of ⅛-scale model.

of circumference and 1/12 of the cylinder length. Solid propellant is represented by constant-strain solid elements in three layers (liftoff condition). A difficulty with this element arises because the solid propellant is essentially incompressible[22] (Poisson's ratio $\mu = 0.5$). Thus, the stress-strain relationship becomes singular because of certain terms with 1-2 μ in their denominator. The problem was circumvented by taking $\mu = 0.4$ (Ref. 12). This finite-element representation was adequate for relatively simple modes of vibration but deteriorated rapidly when modes were dominated by complex shell motions. A much more efficient way of calculating the relatively simple beamlike behavior was obtained with a modified beam representation.

The modified beam model for the SRB was obtained by defining two coincident beams connected to each other at each grid point with springs. The intent was to allow relative motion between the propellant and the case. Thus, the "outer" beam derived its stiffness from the case properties and a small portion of the propellant while the "inner" beam derived its structural dynamic properties from the propellant. This representation of the SRB model was used for the mated model study.

In addition, the SRA program was applied to the SRB models and excellent correlations with experiment were realized for the midburn and near-burnout weight conditions.[12]

Orbiter

The orbiter finite-element model, Fig. 5c, consists of five substructures: fuselage, wing, payload bay door, fin, and simulated payload (not shown). The NASTRAN substructuring capability was used extensively for the orbiter element. Most external surfaces are modeled with membrane elements to allow in-plane deformations in tension, compression, and in-plane shear. Internal components that are modeled with membrane elements include the forward cabin ballast, keel, and top cover of the wing carry-through structure. Some panels of the cargo-bay door are modeled with plate elements which allow both in-plane and bending deformations. Consistent with full-scale shuttle design, the model cargo-bay doors carry fuselage torsion loads but do not support fuselage bending loads. Several modifications to this finite-element model were made during correlation with experimental data.[13]

The final orbiter finite-element model was used as a basis to derive a beam model needed in the mated vehicle analyses. Derivation of the reduced (beam) model was necessary because of the large number of degrees-of-freedom in the four-body finite-element model. The beam model incorporated all significant orbiter structural dynamic characteristics and was used during studies of the two- and four-body configurations.

Typical frequencies and damping

Frequency, Hz		Damping C/C_c, percent		
Sine	Random	Kennedy -Pancu	Log dec.	Random
16.60	16.60	0.45	0.46	0.37
17.50	17.65	.23	.55	.35
20.59	20.67	.40	.65	.48

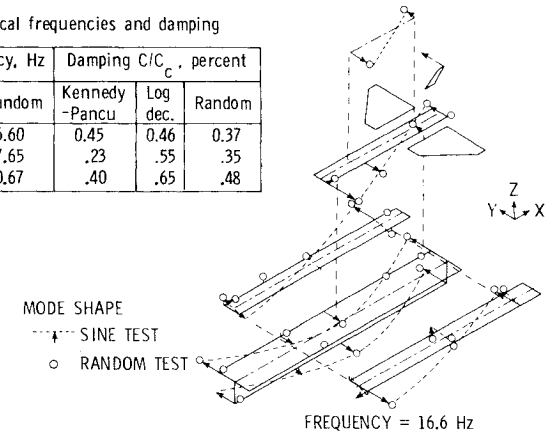

Fig. 6 Comparison of sine and random test results.

Assembled Model Analysis

The manner in which model elements are interconnected results in significant structural dynamic effects. Although the actual connecting links for the ⅛-scale model are very rigid, relatively large deformations can occur in element structure surrounding these links. From a practical standpoint, these large concentrations of forces and associated deformations at interfaces cause difficulty in the verification of element mathematical models. Modal tests of elements are almost always performed with the interfaces free (free-free test) for convenience. Because structure in the critical interface areas is not loaded during these tests, this portion of the mathematical model is not fully verified. The deformation near the interfaces takes place in a localized way so that inertial effects are relatively minor. Therefore a method for verification of element mathematical models was devised in which free-free modes and frequencies for the elements are found for correlation with analysis and, in addition, static tests are performed in which detailed measurements are made and forces or constraints are applied at the element interfaces. Results from these static tests are used to verify a static analysis in which these areas are represented in great detail. With this static analysis, equivalent springs may be derived for coupling the various element mathematical models in an analysis of the assembly.

For the ⅛-scale model, beam models, as discussed previously, were derived to represent overall element structural dynamic behavior. Interconnections of these beam models were made with springs which were derived from finite-element models which had been verified in element static tests. Thus, a relatively simple way of representing overall element dynamics, as well as the critical local deformations, was devised which was compatible with standard vibration test practice. This test-analysis procedure for correlation is based upon ideas in Refs. 23-26.

Results and Discussion

Data from analysis and tests of the ⅛-scale space shuttle dynamic model are presented in Figs. 6-13 and Tables 2 and 3. Sinusoidal test and random test results are compared, the problem area of liquid-structure interaction is addressed, typical damping results are presented, the influence of local deformations at element interfaces is demonstrated, and effects of panel imperfections on stiffness are shown. Finally, a comparison of frequencies for elements and the assembled model configuration at the liftoff mass condition is presented.

Table 2 One-eighth-scale SRB model experimental and analytical structural damping coefficients (liftoff mass)

Type	n	m	Experimental Left	Experimental Right	Analytical finite-element beam model[a] Ref. 9	Analytical finite-element beam model[a] Ref. 12
1st longitudinal	0	1	0.174	0.166	0.180	0.160
1st torsional	0	1	0.056	0.068	0.083	0.070
1st bending	1	2	0.009	0.008	0.030	0.020
2nd bending	1	3	0.027	0.026	0.090	0.080
3rd bending	1	4	0.078	0.066	0.168	0.161

[a] Loss factor = 0.5.

Table 3 Selected ⅛-scale model interface distortions, nm/N

Interface[a]	Test	Analysis
Fwd, SRB/ET, longitudinal	17.6	14.3
Fwd, SRB/ET, yaw	116.0	99.9
Fwd, SRB, ET, pitch	157.0	158.0
Fwd, ET/orbiter, pitch	313.0	338.0
Aft, ET/SRB, longitudinal	152.0	115.0
Aft, ET/SRB, yaw	21.5	21.9
Aft, ET/SRB, pitch	18.0	20.9

[a] Underline denotes the side of the connection investigated.

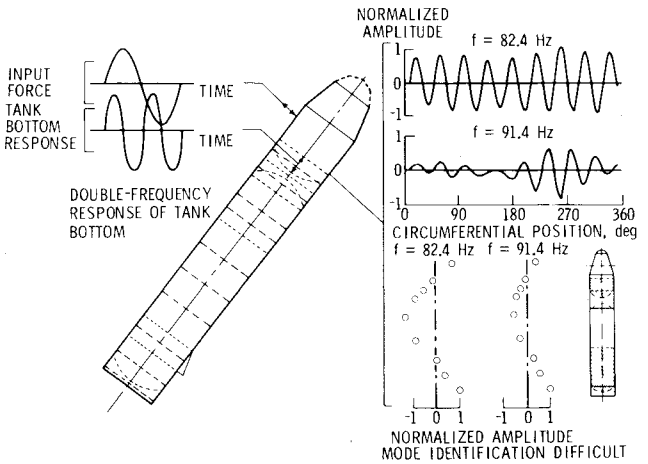

Fig. 7 Observations from liquid-structure testing of model ET and lox tank.

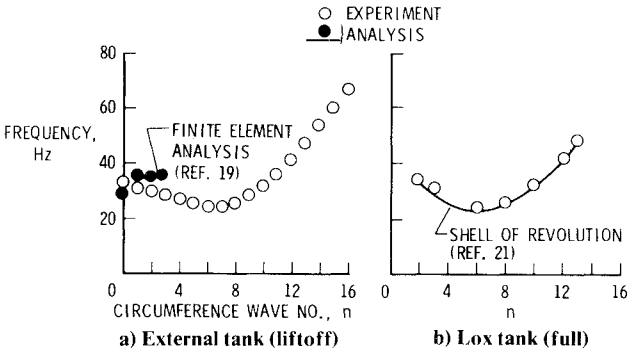

Fig. 8 Comparison of NASTRAN analysis results with experiment for the model ET and shell-of-revolution analysis with experiment on lox tank.

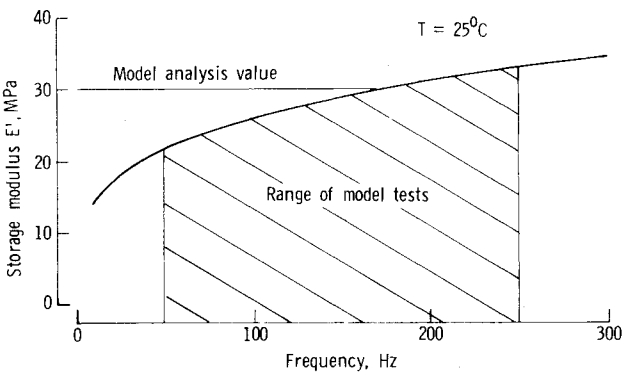

Fig. 9 Storage modulus for model solid propellant.

Comparison of Sinusoidal and Random Test Results

A typical comparison of modal data obtained with the random excitation approach and the more conventional sinusoidal test is shown in Fig. 6. As shown, there is good agreement between measured frequencies, mode shapes, and damping. These comparisons are typical, except for the case of modes in which natural frequencies are in very close proximity. These closely spaced modes require examination of the data with greater frequency resolution in the vicinity of involved resonances. Refinements and data-handling techniques still are being investigated. The random excitation method appears, however, to be suitable for shuttle-like structures based on a comparison of results with those of standard sinusoidal test techniques.

Liquid-Structure Interaction

Because of shell-liquid interaction, many highly complex modes occur in the ET model. Problem areas (Figs. 7 and 8) related to interaction of liquid with the containing structure are mode identification, parametric response, and mathematical modeling.

With respect to difficulties in mode identification, Fig. 7 shows two experimental modes which have characteristics similar to a first-beam bending mode of the ET element. Circumferential surveys in the lox tank area show responses in two shell modes—one with nine full waves circumferentially and one with eight full waves. This is an example of data which shows that description of the dynamic behavior of the ET element in the context of beam-type responses is inadequate. Such structures must be characterized within the framework of shell dynamic behavior.

Another problem area, depicted schematically in Fig. 7, is parametric response. Parametric response is a phenomenon characterized by responses at frequencies which are multiples of two from the input frequency. As suggested in Fig. 7, in separate lox tank component tests prominent responses of the tank bottom were observed at twice the driving frequency. The input force was applied in the cylindrical portion of the tank. This observation is not new for liquid-containing tanks.[27] A significant nonlinear dynamic behavior exists, however, which current practical analysis methods do not treat. Implications of such a dominant response for pogo stability, for example,[28] are not known.

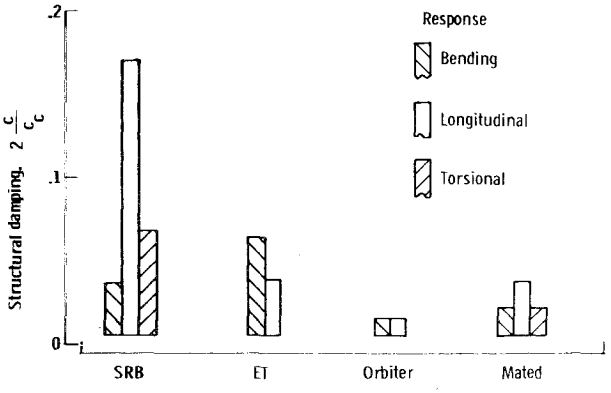

Fig. 10 Range of measured structural damping coefficients.

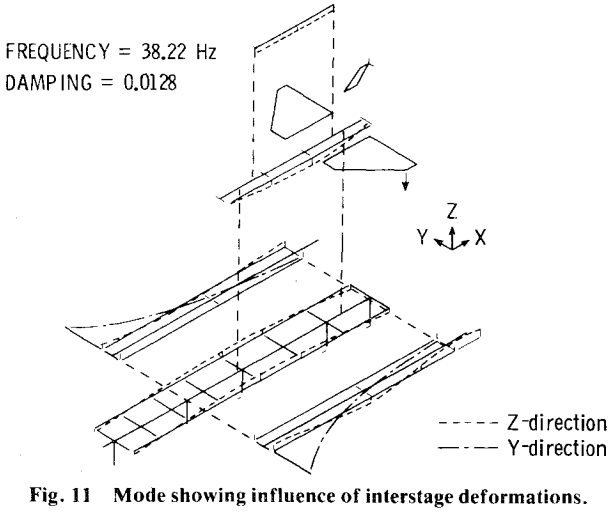

Fig. 11 Mode showing influence of interstage deformations.

A third problem area is finite-element modeling. Existing finite-element codes were found to be inadequate for modeling liquid-structure interaction because the grid needed for a converged solution led to a problem size which exceeded computing capacity. The procedure of Ref. 19 results in system matrices equal in size to those of the structure without fluid. When applied to the ⅛-scale model ET, an order of magnitude reduction in CPU time resulted for extraction of 128 frequencies and 25 mode shapes. Experimental results, Fig. 8a, indicate that even with these theoretical advances there is a need for a better representation circumferentially. As shown on the figure, there is relatively good correlation between the more efficient liquid-structure analysis[19] and test data from the ET only for low circumferential wave numbers ($n = 0 - 2$). The modified SRA analysis, a shell-of-revolution analysis,[21] was applied to the lox tank alone with the result shown in Fig. 8b. Comparison of this result with experimental data is excellent. This analysis, however, is not applicable to the full-scale structure because of the nonaxisymmetric stiffness characteristics of the full-scale hardware.

Damping

The SRB's differ from the other structural elements of the model because of the viscoelastic solid propellant. As part of the element studies, linear finite-element mathematical models with damping were used to approximate this characteristic. To incorporate the viscoelastic properties in a linear analysis, the effective propellant material moduli must be defined. In a viscoelastic material both the tensile and the shear moduli are complex functions of frequency of the applied force. Thus, for tensile modulus, for example,

$$E_p(\omega) = E_p'(\omega) + iE_p''(\omega)$$

where E_p' is termed the storage modulus and E_p'' is termed loss modulus. In addition to frequency, the properties show a dependence on temperature and humidity. Tests were conducted on material samples[22] and selected results are shown in Fig. 9. The figure shows the dependence of the storage modulus on frequency. The value used in the present studies[12] is shown on the figure. Test data showed that the material is essentially incompressible so that Poisson's ratio μ is 0.5. The loss modulus is roughly half the storage modulus. Samples of the propellant should be chosen for testing, if possible, from the same batch used in the casting.

The propellant viscoelastic properties were used in the beam model discussed previously to predict modal damping in the SRB's. The comparison is shown in Table 2. In the first longitudinal and torsional modes the damping values were predicted quite accurately, while the bending mode damping correlation was poor.

Overall structural damping is also of interest. A summary of measured structural damping for the model elements and for the model assembly is presented in Fig. 10. This bar graph shows ranges of measured damping data for bending, longitudinal, and torsional responses in the lower frequency range (the bottoms of the bars indicate minimum measured values). Note the relatively large damping associated with the longitudinal response of the SRB element, the torsional responses of the SRB, and the bending response of the ET elements. The large SRB longitudinal damping (approximately 17%) and the SRB torsional mode damping (approximately 6.5%) can be attributed to the shearing action of the solid propellant when the model is vibrating in these modes. The large damping for the ET in a bending mode is a result primarily of energy being absorbed in the model structural joints. Damping values measured on the orbiter element are quite low, whereas the damping values from SRB propellant shear action were not obtained on the mated model because these modes did not occur in the frequency range of the mated model tests.

Element Interface Distortions

Figure 11 shows a symmetric mode in which the SRB elements act as flexible bodies in yaw with local deformations of the ET and SRB's near the element interfaces. The mode involves element elastic deformation (i.e., lateral bending of the SRB's out-of-phase), but the mode would not be as predominant except for deformation in the ET structure near the SRB-ET forward connection.

A series of static tests and analyses were conducted with the ⅛-scale shuttle model as part of the coupling procedure discussed previously to determine the predictability of the model interface local distortions. Table 3 shows good agreement between some measured and calculated data. To obtain these results, very detailed mathematical representations of the structure near element interfaces were necessary. The forward skirt of the SRB, for example, was represented near the connection point with elements subtending 2½ deg of circumference.

Reduced Stiffness Due to Panel Imperfections

Because design of the space shuttle was preliminary at the time of construction of the ⅛-scale shuttle model, replication of structure was not warranted. Consequently, substantial latitude was allowed in selecting model dimensions, such as panel thicknesses and stiffener spacing. One design compromise in the ⅛-scale shuttle model was the omission of sufficient stiffening in the panels of the fuselage and the wings of the orbiter element. Initial data for the orbiter indicated a discrepancy between analytical and test results of about 20% in the first pitch-plane bending mode frequency. Because of this surprisingly large difference, an intensive investigation was conducted.[13] The primary cause of the large disagreement in frequency was reduced in-plane stiffness in the fuselage panels resulting from out-of-plane imperfections

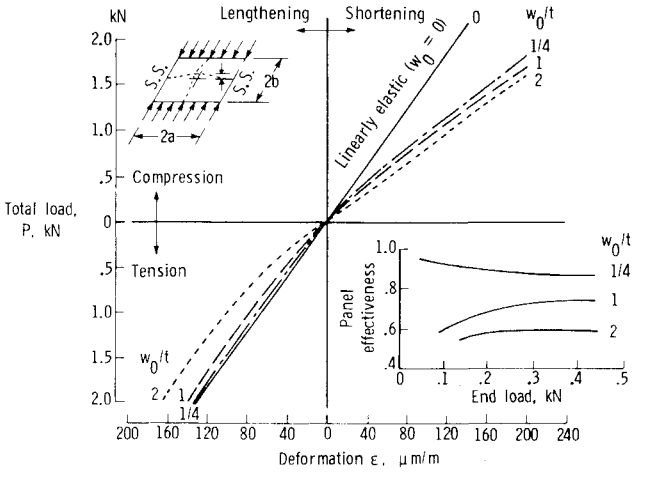

Fig. 12 Reduced stiffness due to panel imperfections.

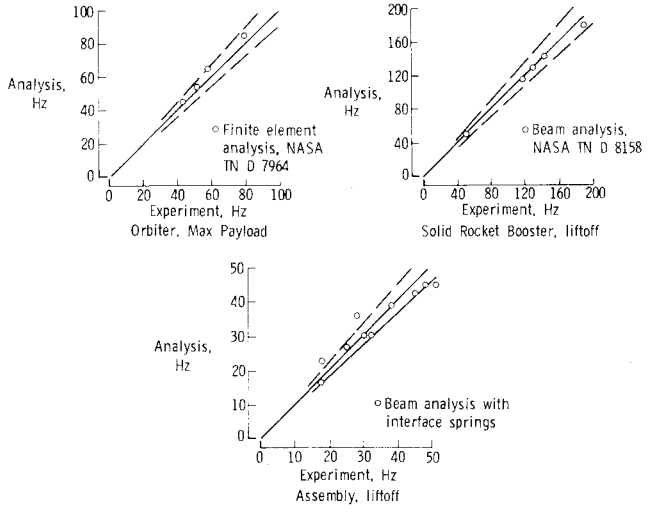

Fig. 13 Model symmetric mode natural frequencies.

of about one to two panel thicknesses. Figure 12 presents load deflection characteristics from a nonlinear analysis of a panel assumed to have a sinusoidally distributed imperfection. The effectiveness, presented as a fraction of the stiffness of the perfect panel, is shown in the inset. As the figure shows, imperfections as large as those observed in the model orbiter element result in stiffness of approximately 60% of the fully effective panel. After accounting for these effects (and effects of joint flexibility which were less important), results of analysis and test correlated well.[13]

Analysis-Test Comparisons

Some correlations between analysis and test for specific purposes have been presented including limited test and analysis results for the ET. Overall results for the other model elements and the assembly are shown in Fig. 13. The graphs in the figure are plots of analysis frequency on the ordinate vs experiment frequency on the abscissa. Perfect correlation for a mode would plot on the 45 deg line shown on each graph. Lines indicating differences of 10% are also shown. Antisymmetric modes were defined experimentally but only limited correlation with analysis was performed. Consequently, only modes symmetric with respect to the pitch plane are shown.

Results for the orbiter element (upper left, Fig. 13) are those corrected for panel imperfection effects discussed previously. Agreement is shown to be within 10% for the four symmetric modes shown. Similar agreement was found for antisymmetric modes.[13]

Shown in the upper right are correlations for the SRB element. A modified beam theory predicts the modes of the SRB's well. Other studies using a shell-of-revolution code and finite-element shell models with different weight conditions are presented and discussed in Ref. 12. Results of these studies indicate finite-element beam-and-plate models can effectively predict membrane, bending, and lower shell modes. For higher shell modes, more refined finite-element or shell-of-revolution analyses are needed.

Results for the liftoff condition of the model assembly are shown in the lower part of the figure. Analysis results are calculated with interface springs connecting beam representations of the model elements as discussed previously. Interface springs are derived from detailed static analyses. The correlation is considered good. However, of the ten modes shown, three exhibited disagreement greater than 10%. There are many more modes over the frequency range than exhibited by the elements individually (17 symmetric and antisymmetric modes in the frequency range 0-50 Hz). This number is regarded as a high density of modes, since this range of frequencies for the full-scale launch vehicle is 0-6 Hz, a range of interest in consideration of launch vehicle structural dynamics problems. For comparison purposes, although not presented herein, calculations were made on the assembled model using beam representations for the elements connected rigidly at the interfaces. Three modes are predicted in the frequency range of interest with the use of flexible interface connections which are not predicted by the analysis having rigid interface connections. These three modes correlate well with experiment, thus showing the necessity for accounting for interface flexibility.

Concluding Remarks

A ⅛-scale dynamic model of an early concept of the space shuttle launch vehicle has been investigated for vibration characteristics. Experimental observations include high density of modes, a wide range of damping in the solid rocket boosters, parametric responses in the lox tank model, and difficulties in modal identification in the external tank because of shell vibration modes. In limited test studies, single-point random excitation test data were shown to correlate well with standard sinusoidal techniques.

Vibration analyses of individual components and the assembly have been compared with test results with correlation generally within 10%. Good correlation required a thorough treatment of the local flexibilities in structure near element interfaces and an account for significant stiffness reductions in the orbiter element due to panel imperfections. For the external tank study, although significant analysis developments have been made to lessen computation time required for accurate modal calculations, practical finite-element solutions can be realized only for a few circumferential waves. An advanced shell-of-revolution analysis, however, gave good correlation with tests. Observed parametric response phenomena are not included in present analyses. Except for local flexibilities, overall solid rocket booster characteristics can be represented faithfully with beam models. A singularity is encountered when the solid element is used to represent the solid propellant which is relatively incompressible. This suggests that a complementary energy approach is more appropriate for such analyses. Prediction of damping in the solid rocket boosters was successful only for very simple modes.

References

[1] Runyan, H.L., Morgan, H.G., and Mixson, J.S., "Use of Dynamic Models in Launch Vehicle Development," AGARD Report 479, May 1964.

[2] Guyett, P.R., "The Use of Flexible Models in Aerospace Engineering," British Royal Aeronautical Establishment, Tech. Rept. 66335, Nov. 1966.

[3] Mixson, J.S., and Catherines, J.J., "Comparison of Experimental Vibration Characteristics Obtained from 1/5-Scale Model and from a Full-Scale Saturn SA-1," NASA TN D-2215, 1964.

[4] Peele, E.L., Thompson, W.M., Jr., and Pusey, C.G., "A Theoretical and Experimental Investigation of the Three-Dimensional Vibration Characteristics of a Scaled Model of an Asymmetrical Launch Vehicle," NASA TN D-4707, Aug. 1968.

[5] Leadbetter, S.A. and Raney, J.P., "Model Studies of the Dynamics of Launch Vehicles," *Journal of Spacecraft and Rockets*, Vol. 3, June 1966, pp. 936-938.

[6] Pinson, L.D. and Leonard, H.W., "Longitudinal Vibration Characteristics of 1/10-Scale Apollo/Saturn V Replica Model," NASA TN D-5159, April 1969.

[7] Grimes, P.J., McTigue, L.D., Riley, G.F., and Tilden, D.I., "Advancements in Structural Dynamic Technology Resulting from Saturn V Programs. Vol. I," NASA CR-1539, June 1970.

[8] Grumman Aerospace Corp., "Design of Space Shuttle Structural Dynamics Model," NASA CR-112205, 1972.

[9] Levy, A., Zalesak, J., Bernstein, M., and Mason, P.W., "Development of Technology for Modeling of a ⅛-Scale Dynamic Model of the Shuttle Solid Rocket Booster (SRB), NASA CR-132492, July 1974.

[10] Bernstein, M., Coppolino, R., Zalesak, J., and Mason, P.W., "Development of Technology for Fluid-Filled Structure Interaction Modeling of a ⅛-Scale Dynamic Model of the Shuttle External Tank (ET)," NASA CR-123549, Vol. I, Technical Report, Vol. II, Supporting Data, Appendices A-C, 1974.

[11] Mason, P.W., and Harris, H.G., Zalesak, J., and Bernstein, M., "Analytical and Experimental Investigation of the ⅛-Scale Dynamic Model of the Shuttle Orbiter," NASA CR-132488, Vol. I, Summary Report; NASA CR-132489, Vol. II, Technical Report; NASA CR-132490, Vol. IIIA, Supporting Data; NASA CR-132491, Vol. IIIB, Supporting Data, 1974.

[12] Leadbetter, S.A., Stephens, W.B., Sewall, J.L., Majka, J.W., and Barrett, J.R., "Vibration Characteristics of ⅛-Scale Dynamic Models of the Space Shuttle Solid Rocket Boosters," NASA TN D-8158, May 1976.

[13] Pinson, L.D., "Coordinator: Analytical and Experimental Vibration Studies of ⅛-Scale Shuttle Orbiter," NASA TN D-7964, 1975.

[14] Blanchard, U.J., Miserentino, R., and Leadbetter, S.A., "Experimental Investigation of the Vibration Characteristics of a Model of an Asymmetric Multielement Launch Vehicle," NASA TN D-8448, Sept. 1977.

[15] Schoenster, J.A., "Measured and Calculated Vibration Properties of Ring-Stiffened Honeycomb Cylinders," NASA TN D-6090, 1971.

[16] Keller, A.C., "Vector Component Techniques: A Modern Way to Measure Modes," *Sound and Vibration*, Vol. 3, March 1969, pp. 18-26.

[17] Salyer, R.A., Jung, E.J., Jr., Huggins, S.L., and Stephens, B.L., "An Automatic Data System for Vibration Modal Tuning and Evaluation," NASA TN D-7945, 1975.

[18] Richardson, M. and Potter, R., "Identification of the Modal Properties of an Elastic Structure from Measured Transfer Function Data," *Proceedings of the 20th International Instrumentation Symposium*, Albuquerque, N. Mex., 1974

[19] Coppolino R.N., "A Numerically Efficient Finite Element Hydroelastic Analysis, Vol. I: Theory and Results," Grumman Aerospace Corp., NASA CR-2662, 1976.

[20] Archer, J.S. and Rubin, C.P., "Improved Analytic Longitudinal Response Analysis for Axisymmetric Launch Vehicles, Volume I—Linear Analytic Model," TRW Space Technology Labs., NASA CR-345, 1965.

[21] Housner, J.M. and Herr, R.W., "Vibrations of Incompressible Liquid Elastic Tank Combinations Using a Series Representation of the Liquid," Symposium on Computing Methods in Fluid Structural Response Problems—Winter Annual Meeting of ASME, Nov.-Dec. 1977, Atlanta, Ga.

[22] Hufferd, W.L., "Measured Properties of Propellant for Solid Rocket Booster of ⅛-Scale Dynamic Shuttle Model," NASA CR-144938, 1976.

[23] Kuhar, E.J. and Stahle, C.V., "Dynamic Transformation Method for Modal Synthesis," *AIAA Journal*, Vol. 12, May 1974, pp. 672-678.

[24] MacNeal, R.H., "A Hybrid Method of Component Mode Synthesis," *Journal of Computers and Structures*, Vol. 1, Dec. 1971, pp. 581-601.

[25] Rubin, S., "Improved Component-Mode Representation for Structural Dynamic Analysis," *AIAA Journal*, Vol. 13, Aug. 1975, pp. 995-1006.

[26] Craig, R., Jr. and Chang, C.J., "On the Use of Attachment Modes in Substructure Coupling for Dynamic Analysis," Paper 77-405, AIAA/ASME 18th Structures, Structural Dynamics and Materials Conference, March 1977, San Diego, Calif.

[27] Kana, D.D., "Parametric Oscillations of a Longitudinally Excited Cylindrical Shell Containing Liquid," Final Rept., Proj. 02-1786 (IR), Southwest Research Institute, San Antonio, Tx., Jan. 1967.

[28] Anon., "Prevention of Coupled Structure—Propulsion Instability (Pogo)," NASA Space Vehicle Design Criteria (Structures), NASA SP-8055, 1970.